Stoichiometric O_2 Oxidation of Bis(Thioether)(Octaethylporphyrinato)ruthenium(II) Complexes to the Corresponding Sulfoxide Species in Acidic Media. Structural Confirmation of S-Bonded Sulfoxides

Andrew Pacheco, Brian R. James,* and Steven J. Rettig†

Department of Chemistry, University of British Columbia, Vancouver, BC, Canada V6T 1Z1

Received July 9, 1999

Exposure to O_2 (or air) of a CH_2Cl_2, benzene, or toluene solution containing $PhCO_2H$ and $Ru(OEP)(RR'S)_2$ (where OEP = the dianion of 2,3,7,8,12,13,17,18-octaethylporphyrin, R = methyl, ethyl, or decyl, and R′ = methyl or ethyl), at ambient conditions, results in the selective oxidation of the axial ligand(s) on the metalloporphyrin complex to the corresponding sulfoxide(s). For example, a CD_2Cl_2 solution of $Ru(OEP)(dms)_2$ (dms = dimethyl sulfide) and $PhCO_2H$, exposed to 1 atm of O_2 at ∼20 °C for 35 h, is oxidized to $Ru(OEP)(dmso)_2$, and the intermediates Ru(OEP)(dms)(dmso), $[Ru(OEP)(dms)_2][PhCO_2]$, and $Ru(OEP)(dms)(PhCO_2)$ are identified (*s* implies sulfur-bonded). Mechanisms invoking in situ formation of H_2O_2, disproportionation of Ru^{III} species, and Ru^{IV}═O intermediates are proposed for the O_2 oxidation of the thioether ligands. X-ray analysis of $Ru(OEP)(Et_2SO)_2$ confirms that the sulfoxides are S-bonded.

Introduction

Studies from this group have reported previously on the selective O_2 oxidation of thioethers to sulfoxides using the sterically hindered *trans*-dioxo species $Ru(TMP(O)_2$ and $Ru(OCP)(O)_2$;[1] these reactions occur via O-atom transfer processes via the Ru^{VI}(dioxo) species with involvement of Ru^{IV}(oxo) species.[2−4] We have also noted earlier that complexes such as $Ru(OEP)(RR'S)_2$, with a non sterically hindered porphyrin, also catalyze the autoxidations of thioethers under certain conditions.[5,6] Such thioether oxidations are important commercially.[2,7] We report here on the mechanism of the stoichiometric O_2 oxidation of $Ru(OEP)(RR'S)_2$ complexes, which provides a framework for understanding the catalytic autoxidation of thioethers to sulfoxides using such nonhindered species.[8]

Our previous studies have shown that when solutions of $Ru(OEP)(RR'S)_2$ were exposed to air for weeks, the complexes underwent slow ligand oxidation to give mainly Ru(OEP)(RR′S)(RR′*S*O) and $Ru(OEP)(RR'SO)_2$, along with other minor products.[5,9] The degree of reactivity of the complex and the product distribution were variable and depended on the thioether, the solvent, and particularly the dryness of the solvent. However, air oxidation of an *acidic* solution of $Ru(OEP)(RR'S)_2$ showed reproducible generation of the corresponding sulfoxide complexes either in benzene, toluene, or CH_2Cl_2, and several intermediates were observed. In an earlier paper,[6] we described the syntheses of the $Ru(OEP)(RR'S)_2$, $Ru(OEP)(RR'SO)_2$, $[Ru(OEP)(RR'S)_2]^+$, and $[Ru(OEP)(PhCO_2)_2]^-$ species to be discussed in the present paper.

Experimental Section

The instrumentation, materials, and methods used for the experiments are generally described in ref 6, which also details the syntheses of $Ru(OEP)L_2$ (L = dms, Et_2S, decMS, or the corresponding sulfoxides), $[Ru(OEP)L_2][BF_4]$ (L = dms, Et_2S, or decMS), and $[Me_4N][Ru(OEP)(PhCO_2)_2]$. All solvents were thoroughly predried; CD_2Cl_2 was dried over 3 Å molecular sieves, while hydrocarbon solvents were dried over sodium−benzophenone. Unless exposure to O_2 was expressly desired, all manipulations of Ru(OEP) complexes were performed under Ar or in vacuo.

A typical O_2-oxidation experiment was initiated by breaking open an NMR tube, previously sealed in vacuo and containing the desired reaction mixture, in a stream of O_2 (Union Carbide of Canada, USP grade, used without further purification). For the experiment described in most detail below, a CD_2Cl_2 solution (∼0.5 mL) containing ∼10 mM $Ru(OEP)(dms)_2$ and ∼10 mM $PhCO_2H$ was prepared in vacuo, in an NMR tube fitted with a coaxial Teflon valve (Wilmad *Roto Tite*). After the $t = 0$ spectrum was obtained in vacuo, the experiment was initiated by opening the valve in a darkened room and exposing the reaction mixture to 1 atm of O_2 (US Airweld), thoroughly dried by a column of Sicapent (a P_2O_5-based drying agent). After the Teflon valve was reclosed, the NMR tube was vigorously shaken to dissolve the O_2 in the solution and then was inserted into the 300 MHz NMR instrument, thermostated at 23.0 °C. Spectral changes were monitored for ∼12 h before the tube was removed from the instrument, shaken, and stored in the dark at 23 °C; further spectra were collected after ∼22 and 40 h. Of note, the results obtained in this specific experiment did not differ significantly from those obtained using the somewhat less rigorous method described above, or when concentrations of Ru and acid were varied. The experiments do not constitute a rigorous kinetic study, primarily because of the difficulty in maintaining a constant $[O_2]$ in solution within the NMR tube.

* To whom correspondence should be addressed.
† Deceased on October 27, 1998.

(1) Abbreviations used: TMP, dianion of *meso*-tetramesitylporphyrin; OCP, dianion of *meso*-tetra(2,6-dichlorophenyl)porphyrin; OEP, dianion of 2,3,7,8,12,13,17,18-octaethylporphyrin; Por, a generic porphyrin; dms, dimethyl sulfide; dmso, dimethyl sulfoxide (*s* or *o* within an abbreviation for any sulfoxide ligand implies S- or O-bonded, respectively); decMS, *n*-decyl methyl sulfide; decMSO, *n*-decyl methyl sulfoxide; R, methyl, ethyl, or decyl; R′, methyl or ethyl; CV, cyclic voltammetry.

(2) Rajapakse, N.; James, B. R.; Dolphin, D. *Catal. Lett.* **1989**, *2*, 219; *Stud. Surf. Sci. Catal.* **1990**, *55*, 109.
(3) Mlodnicka, T.; James, B. R. In *Metalloporpyrin-Catalyzed Oxidations;* Montanari, F., Casella, L., Eds.; Kluwer: Dordrecht, The Netherlands, 1994; p 121.
(4) Cheng, S. Y. S.; James, B. R. *J. Mol. Catal. A* **1997**, *117*, 91.
(5) James, B. R.; Pacheco, A.; Rettig, S. J.; Ibers, J. A. *Inorg. Chem.* **1988**, *27*, 2414.
(6) Pacheco, A.; James, B. R.; Rettig, S. J. *Inorg. Chem.* **1995**, *34*, 3477.
(7) Hill, C. L.; Gall, R. D. *J. Mol. Catal. A* **1996**, *114*, 103.
(8) (a) Pacheco, A. A. Ph.D. Dissertation, The University of British Columbia, Vancouver, BC, 1992. (b) Pacheco, A.; James, B. R. To be published.
(9) Pacheco, A. A. M.Sc. Dissertation, The University of British Columbia, Vancouver, BC, 1986, and unpublished data.

10.1021/ic9908219 CCC: $18.00
Published on Web 11/10/1999

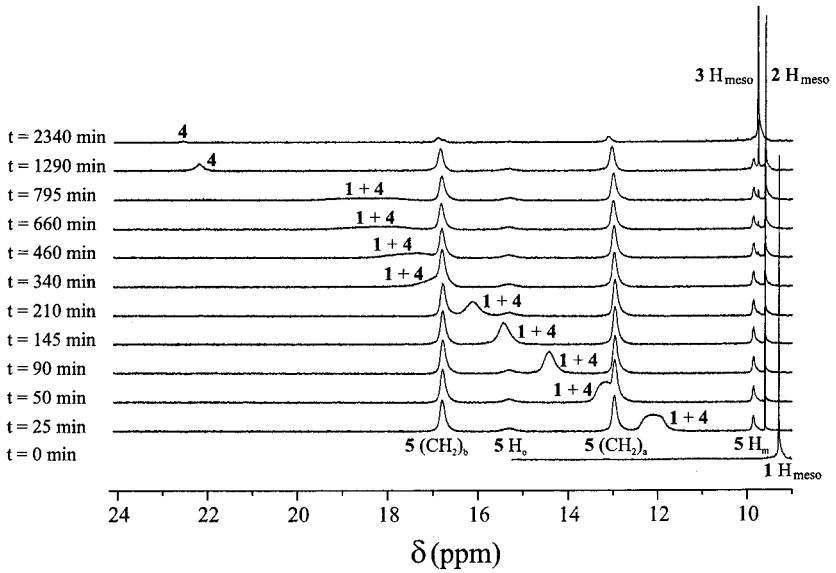

Figure 1. Selected ^{1}H NMR spectral changes over time (min) after an acidic CD_2Cl_2 solution of Ru(OEP)(dms)$_2$ (**1**) is exposed to 1 atm of O_2 at 23.0 °C; **2** is Ru(OEP)(dms)(dmso), **3** is Ru(OEP)(dmso)$_2$, **4** is [Ru(OEP)(dms)$_2$]$^+$, and **5** is Ru(OEP)(dms)($PhCO_2$). The complete spectra are provided as Supporting Information, and the corresponding peak assignments for each species are summarized in Table 2.

Table 1. Crystallographic Data[a]

compound	Ru(OEP)(Et_2SO)$_2$
formula	$C_{44}H_{64}N_4O_2S_2Ru$
fw	846.21
cryst syst	monoclinic
space group	$P2_1/n$
a, Å	10.235(2)
b, Å	10.224(1)
c, Å	20.796(1)
β, deg	95.454(8)
V, Å^3	2166.2(4)
Z	2
ρ_{calc}, g/cm^3	1.297
T, °C	21
radiation	Cu
λ, Å	1.541 78
μ, cm^{-1}	41.34
trans factors (rel)	0.61−1.00
$R(F)$	0.042
$R_w(F)$	0.046

[a] $R = \sum||F_o| - |F_c||/\sum|F_o|$, $R_w = (\sum w(|F_o| - |F_c|)^2/\sum w|F_o|^2)^{1/2}$.

X-ray Crystallographic Analysis of Ru(OEP)(Et_2SO)$_2$. Crystals of Ru(OEP)(Et_2SO)$_2$ suitable for X-ray analysis were obtained by slow evaporation of a solution initially containing ~5 mM Ru(OEP)(Et_2SO)$_2$ and ~1 M Et_2SO in benzene. Selected crystallographic data appear in Table 1. The final unit-cell parameters were obtained by least-squares on the setting angles for 25 reflections with $2\theta = 71.3-89.5°$. The intensities of three standard reflections, measured every 200 reflections throughout the data collection, showed only small random fluctuations. The data were processed[10] and corrected for Lorentz and polarization effects and absorption (empirical, based on azimuthal scans).

The structure was solved by conventional heavy-atom Patterson methods and was refined by full-matrix least-squares procedures to $R = 0.042$ ($R_w = 0.046$) for 3332 reflections with $I \geq 3\sigma(I)$. The Ru atom lies on a crystallographic inversion center. The Et_2SO ligand was modeled as 2-fold disordered (83:17) with respect to rotation about the Ru−S bond. In addition the β carbons of the ethyl groups were further disordered. The S atom itself may also be disordered, but the components could not be resolved. The internal geometry of the Et_2SO ligand is unreliable as a result of the disorder. The 0.17-occupancy O and C atoms were refined with isotropic thermal parameters, while the remaining non-hydrogen atoms were refined with anisotropic thermal parameters. Hydrogen atoms (except those associated with the 0.17-occupancy components of the disordered ethyl groups) were fixed in calculated positions (C−H = 0.98 Å and $B_H = 1.2B_{bonded\ atom}$). A correction for secondary extinction (Zacharaisen type) was applied, the final value of the extinction coefficient being 2.29(9) $\times 10^{-6}$. Neutral atom scattering factors for all atoms[11] and anomalous dispersion corrections for the non-hydrogen atoms[12] were taken from standard sources. A complete table of crystallographic data, atomic coordinates and equivalent isotropic thermal parameters, hydrogen atom parameters, anisotropic thermal parameters, bond lengths, bond angles, torsion angles, intermolecular contacts, and least-squares planes are included as Supporting Information (Tables S1−S8). The crystal structure confirms that the Ru(OEP)($RR'SO$)$_2$ complexes contain S-bonded ligands as suggested earlier by IR and NMR data.[6]

Results and Discussion

Reaction of Ru(OEP)(dms)$_2$ (1) with O_2 and $PhCO_2H$ in CH_2Cl_2. Figure 1 shows the ^{1}H NMR spectral changes over time after a solution containing ~10 mM **1** and 10 mM $PhCO_2H$ in CD_2Cl_2 is exposed to 1 atm of O_2 at room temperature (23.0 °C). For simplicity only part of the spectrum is shown, but corresponding changes are seen throughout the spectrum, from δ −3 to 25 (see Table 2 and Supporting Information, Figure S1). When the Et_2S or decMS bis-thioether complexes are exposed to the same conditions, spectral changes analogous to those illustrated in Figure 1 are observed, at least in the δ 5−25 region; at $\delta < 5$, the spectra of the reaction mixtures are too complicated to interpret readily.

The sharp singlet at δ 9.60 is due to the meso proton of Ru(OEP)(dms)(dmso) (**2**), and that at δ 9.78 is similarly assigned to Ru(OEP)(dmso)$_2$ (**3**).[6] Although **2** could not be obtained pure, in titrations of **1** with dmso, or of **3** with dms, the mixed species could be unequivocally identified by ^{1}H NMR (Figure 2). Separate signals are observed at δ −2.07 and −2.87 for coordinated dmso and dms, respectively, and the presence of the multiplet for the OEP methylenes shows that the complex is not symmetrical about the porphyrin plane.[5,13] Also, for the

(10) *teXsan: Crystal Structure Analysis Package*; Molecular Structure Corporation: The Woodlands, TX, 1995.

(11) *International Tables for X-Ray Crystallography*; Kynoch Press: Birmingham, England, 1974; Vol. IV, pp 99−102.

(12) International Tables for Crystallography; Kluwer Academic Publishers: Boston, MA, 1992; Vol. C, pp 200−206.

(13) James, B. R.; Dolphin, D.; Leung, T. W.; Einstein, F. W. B.; Willis, A. C. *Can. J. Chem.* **1984**, *62*, 1238.

Table 2. The ^{1}H NMR Shifts in CD_2Cl_2 for the Ru(OEP) Complexes Shown in Figure 1[a]

	OEP signals, δ			axial ligand signals, δ				
						$PhCO_2$		
	CH_3	CH_2	H_{meso}	dms	dmso	H_o	H_m	H_p
$Ru(OEP)(dms)_2$ (**1**)	1.81, t	3.85, q	9.32, s	−2.66, s				
Ru(OEP)(dms)(dmso) (**2**)	1.83, t	3.92, m	9.60, s	−2.87, s	−2.07, s			
$Ru(OEP)(dmso)_2$ (**3**)	1.87, t	3.98, q	9.78, s		−2.18, s			
$[Ru(OEP)(dms)_2]^+$ (**4**)[b]	1.52[c]	23.85	1.73	−0.17				
$Ru(OEP)(dms)(PhCO_2)$ (**5**)	0.46	16.75, 12.87	4.07	−0.49		15.34	9.84	8.75
$[Me_4N][Ru(OEP)(PhCO_2)_2]$ (**6**)[d]	−0.72	8.08	2.72			17.86	10.74	9.35

[a] The assignments for species **1**, **3**, **4**, and **6** are discussed in ref 6. [b] The signals are independent of the counterion. [c] All the signals attributed to Ru^{III} complexes are broad and lacking in fine structure. [d] The Me_4N^+ signal is at δ 5.64.

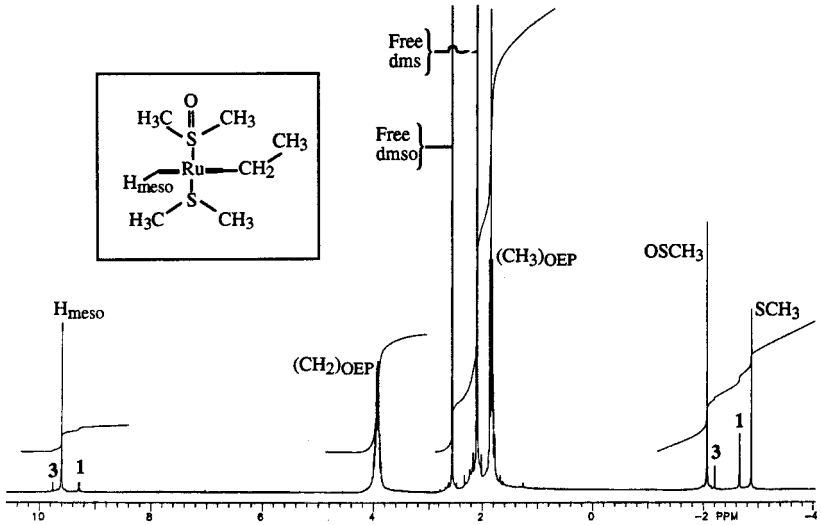

Figure 2. ^{1}H NMR spectrum of a CD_2Cl_2 solution of **1** (~5 mM), dms (~30 mM), and dmso (~10 mM). Under these conditions, the major Ru(OEP) species in solution is **2**, which has a characteristic UV/vis λ_{max} at 403 nm.[8] Some **3** is also present.

Table 3. ^{1}H NMR Signals (δ_{obs}), Assigned to the (**1**)/(**4**) Exchange for the Data of Figure 1 (**1** = $Ru^{II}(OEP)(dms)_2$, **4** = $[Ru^{III}(OEP)(dms)_2]^+$), and the Calculated Remaining Mole Fraction of **1** (N_{II})[a]

	δ_{obs} (N_{II})			
time (min)	CH_3	CH_2	H_{meso}	SCH_3
25	1.69 (0.59)	12.1 (0.59)	6.16 (0.58)	−1.63 (0.59)
50	1.67 (0.52)	13.2 (0.53)	5.74 (0.53)	−1.49 (0.53)
90	1.65 (0.45)	14.4 (0.47)	5.28 (0.47)	−1.33 (0.47)
145	1.64 (0.41)	15.4 (0.42)	4.90 (0.42)	−1.21 (0.42)
210	1.63 (0.38)	16.1 (0.39)	4.64 (0.38)	−1.12 (0.38)
340	1.62 (0.34)	17.1 (0.34)	4.33 (0.34)	−1.01 (0.34)
460	1.61 (0.31)	17.4 (0.32)	4.12 (0.32)	−0.93 (0.31)
660	1.59 (0.24)	18.2 (0.28)	~3.9 (0.3)	−0.83 (0.27)
795	1.59 (0.24)	18.0 (0.28)	~3.9 (0.3)	−0.79 (0.25)
1290	1.54 (0.07)	22.2[b]	2.34 (0.08)	−0.38 (0.08)
2340[c]		22.6[b]		

[a] Calculated by the formula $N_{II} = (\delta_{obs} - \delta_{III})/(\delta_{III} - \delta_{II})$, where δ_{II} and δ_{III} are the δ values for **1** and **4**, respectively. [b] These methylene signals are no longer in the fast-exchange range. [c] Only the methylene signal is still detectable after 2340 min.

analogous system involving Et_2S and Et_2SO, the equilibrium constants as well as the rate constants for the substitution processes have been determined by stopped-flow spectrophotometry.[8]

The broad signal in Figure 1 that shifts over time is one of four, attributable to a time-averaged spectrum of $[Ru(OEP)(dms)_2]^+$ (**4**) and **1** rapidly exchanging via electron transfer; all four peak positions for the spectra collected are listed in Table 3. Figure 3 shows the spectrum of pure **4** within the BF_4^- salt. When this complex was mixed with **1** in CD_2Cl_2, only time-averaged ^{1}H NMR signals could be seen, and the location of all four signals depended exclusively on the concentration ratio of Ru^{III}/Ru^{II}, confirming that electron transfer between **1** and **4** at 20 °C is very rapid (see also below).[14] Of note, the time-averaged OEP methylene signal for **1** and **4** shifts over time towards the Ru^{III} position, showing that the ratio of Ru^{III}/Ru^{II} for the bis-dms species is increasing with time. Table 3 lists the calculated value of the mole fraction, N_{II} ([**1**]/([**1**] + [**4**])), for each spectrum collected. Rapid electron transfer between metal centers of metalloporphyrins of this type is well documented and almost certainly occurs via an outer-sphere process mediated by porphyrin ligand cation radicals.[15] Crystallographic data for $Ru(OEP)(decMS)_2$ and $[Ru(OEP)(decMS)_2]^+$ show no significant difference in corresponding bond lengths or bond angles,[5,6] and thus within these low-spin systems the minimal bond reorganizational energies required are expected to give rapid electron exchange.[16,17]

The shapes of the time-averaged OEP methylene signals of **1** and **4** require some comment. In the first two or three spectra collected, this signal appears noticeably flattened on top, compared to a typical Gaussian or Lorentzian curve. This is attributed to the fact that the signal moved significantly downfield while the spectrum in question was being acquired (the line shape was monitored during acquisition, and became broader as more transients were collected). In the spectra collected between 60 and 300 min, the methylene signal appears normal for a paramagnetic species, indicating a decrease in the

(14) Drago, R. S. *Physical Methods for Chemists*, 2nd ed.; W. B. Saunders: Philadelphia, PA, 1992; Chapter 8.
(15) Castro, C. E. In *The Porphyrins*; Dolphin, D., Ed.; Academic Press: New York, NY, 1978; Vol. V, Chapter 1.
(16) Wilkins, R. G. *Kinetics and Mechanisms of Reactions of Transition Metal Complexes*; VCH: Weinheim, 1991; Chapter 5.
(17) Stynes, H. C.; Ibers, J. A. *Inorg. Chem.* **1971**, *10*, 2304.

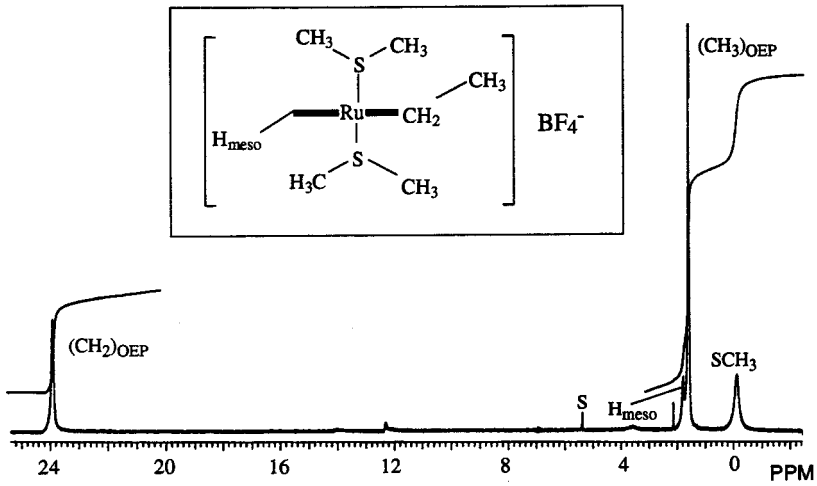

Figure 3. ^{1}H NMR spectrum of [Ru(OEP)(dms)$_2$][BF$_4$] (**4**[BF$_4$]); 20.0 °C in CD_2Cl_2; S = solvent.

rate of downfield motion. However, the signal again appears noticeably broadened in the spectra collected between ~350 and 800 min, before sharpening up again in the last two spectra. This second episode of broadening is not observed for the other signals attributable to the **1** and **4** exchange system. The necessary condition for detecting separate resonances for the proton in each of the Ru^{II} and Ru^{III} environments is given by $\tau > 1/(2^{0.5}\pi\Delta\nu_0)$, where τ is the lifetime of the proton at each site, and $\Delta\nu_0$ is the separation of the peaks (in hertz) in the absence of exchange.[14] For the OEP methylene protons $\Delta\nu_0$ is 20 ppm (see Table 2), i.e., 6000 Hz for the 300 MHz machine used, and thus τ must be less than 3.8×10^{-5} s in the range where separate resonances are not seen. When two proton environments are being exchanged by a second-order process, such as is the case here, the additional condition $k[x] = \tau^{-1}$ (k is the second-order rate constant for the process, and [x] is the concentration of the less abundant of the exchanging species) must hold if separate resonances are not seen.[14] As discussed further below, both [**1**] and [**4**] decrease with time, and the broadening observed between ~350 and 800 min appears to be due to a decrease of [**1**] to a point where the methylene signal begins to slip out of the fast-exchange region. In the range in which the methylene signal is noticeably broadened, [**1**] ~0.5−1 mM, and [**4**] ~ 1.5 mM (see below), which yields a rough estimate of $k \sim 5 \times 10^7$ M^{-1} s^{-1} for the second-order rate constant. None of the other signals attributable to [**1**] and [**4**] is broadened, because $\Delta\nu_0$ is much smaller for these signals, so that they remain in the fast-exchange region throughout the time investigated. Finally, the sharper methylene signals observed after 800 min, now in the slow-exchange regime, must correspond essentially to **4** only.

The signals at δ 12.95 and 16.80 (but shifted slightly downfield in the final two spectra) in Figure 1 are attributed to the OEP methylene protons of the paramagnetic Ru^{III} complex Ru(OEP)(dms)(PhCO$_2$) (**5**) (see Table 2 and below). Two signals are observed because the two different axial ligands make the anisochronous methylene protons magnetically inequivalent.[13] The signals at δ 9.85 and 15.30 in Figure 1 are also attributed to **5** (H_m and H_o of the coordinated benzoate, respectively).

Complexes **1**−**5** account for all of the metalloporphyrin-related ^{1}H NMR signals observed after the exposure of **1** to O_2, with the possible exception of some very minor signals at δ 0.95 and 6.08 seen only in the final spectrum (see Table 2 and Figure S1). In addition to these signals, the complete ^{1}H NMR spectra (Figure S1) also exhibit singlets at δ 2.09 and 2.58, assigned to free dms and dmso, respectively, a cluster of signals centered at δ ~7.5 attributable to free benzoic acid and benzoate (see below), and a broad signal around δ ~6.5 which shifts over time and is discussed further below. On the basis of mass balance and an integral analysis of the corresponding spectra, the product distributions of **1**−**5**, and of free dms, dmso, and benzoate, can be determined as a function of time (Figure 4). By the time the first spectrum was collected, [**1**] had dropped to ~20% of its initial concentration; at this stage the Ru^{III} species **4** and **5** account for ~70% of the total [Ru(OEP)], while **2** accounts for the remaining 10%. Significant amounts of **3** are not seen until ~800 min after exposure to O_2.

The initial rapid production of **4** and **5** is rationalized by the following reaction sequence [*Ru* = Ru(OEP)]:

$$2Ru^{II}(\mathrm{dms})_2\ (\mathbf{1}) + O_2 + 2PhCO_2H \rightarrow 2[Ru^{III}(\mathrm{dms})_2]^+\ (\mathbf{4}) + 2PhCO_2^- + H_2O_2 \quad (1)$$

$$\mathbf{4} + PhCO_2^- \rightleftharpoons Ru^{III}(\mathrm{dms})(PhCO_2)\ (\mathbf{5}) + \mathrm{dms} \quad (2)$$

Step one involves electron transfer from Ru^{II} to O_2 to form Ru^{III} and superoxide stabilized by protons as HO_2, followed by its disproportionation to give H_2O_2 and O_2. We have previously established such a mechanism by detection of HO_2 within related bis(phosphine) complexes of Ru(II).[13,18] The disproportionation is fast and irreversible[19] and would drive reaction 1 to completion. The amounts of *Ru^{III}* species initially generated after exposure to O_2 are almost certainly determined by the amount of O_2 immediately available in solution, as the initial amount of O_2 in the CH_2Cl_2 (~8 mM[20]) is in the range of [**1**]. Under 1 atm of pressure the NMR tube (approximately 4 mL capacity) contains ~30 times more O_2 than is required to eventually oxidize all of **1** to **3**.

If a 10-fold excess of dms is added to a CH_2Cl_2/$PhCO_2H$ solution of **1**, the thermal reaction with O_2 is completely inhibited (catalytic O_2 oxidation of excess dms under corresponding conditions can occur with a visible light source[8]). This implies that an inner-sphere process, with O_2 replacing a bonded dms, occurs prior to electron transfer in reaction 1. There is precedence for such an inner-sphere mechanism as well as for

(18) James, B. R.; Mikkelsen, S. R.; Leung, T. W.; Williams. G. M.; Wong, R. *Inorg. Chim. Acta* **1984**, *85*, 209.
(19) Sawyer, D. T.; Valentine, J. S. *Acc. Chem. Res.* **1981**, *14*, 393.
(20) *IUPAC Solubility Data Series*; Battino, R., Kertes, A. S., Eds.; Pergamon Press: Elmsford, NY, 1981; Vol. 7, p 452.

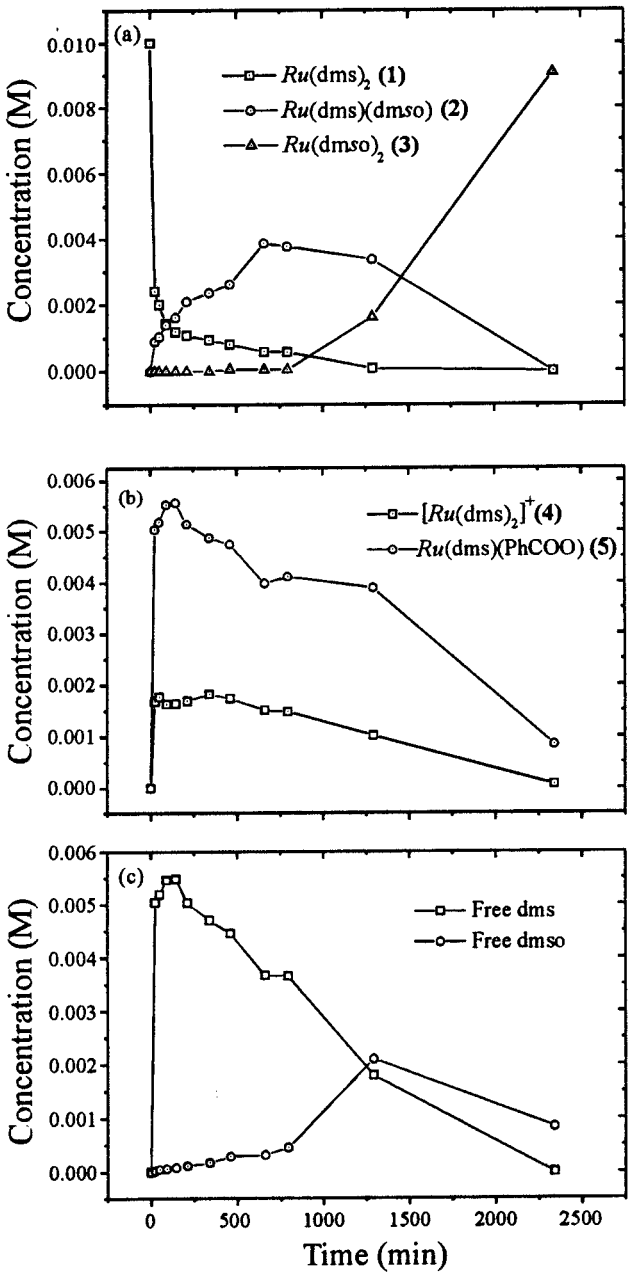

Figure 4. (a, b) Product distributions of **1**−**5**, as a function of time, for the experiment illustrated in Figure 1. (c) Concentrations of free dms and dmso, as a function of time, for the same experiment. At any given time the concentration of free $PhCO_2^-$ should equal that of **4**. The concentrations were determined from mass balance and an integral analysis of the spectra partially shown in Figure 1 and fully provided as Supporting Information (Figure S1). The data are not considered to constitute a rigorous kinetic study (see Experimental Section).

direct outer-sphere electron transfer,[15,21] although the latter is extremely unfavorable in the present system:

$$O_2 + e^- \rightleftharpoons O_2^-, \quad E^\circ = -0.8 \text{ V vs Ag/AgCl (ref 19)}$$

$$\mathbf{4} + e^- \rightleftharpoons \mathbf{1}, \quad E^\circ = 0.22 \text{ V vs Ag/AgCl (ref 6)}$$

These data translate to an equilibrium constant value of about 10^{-17} for the outer-sphere process $Ru^{II} + O_2 \rightleftharpoons Ru^{III} + O_2^-$; protonation and removal of the superoxide can nullify the back reaction of this equilibrium, but the findings imply that in this case outer-sphere electron transfer from Ru^{II} to O_2 must also be kinetically slow.

Experimentally the quotient ([**5**][dms])/([**4**][$PhCO_2^-$]) is found to be reasonably constant (average value 8 ± 2; Figure S2), as required by the equilibrium depicted in eq 2. This implies that **4** and $PhCOO^-$ are sufficiently large and hydrophobic to exist as independent ions (rather than as an ion pair) in CH_2Cl_2 ($\epsilon = 8.93$);[22] of note, the BF_4^- salt of **4** has a molar conductivity of 66 Ω^{-1} cm^2 mol^{-1}, compared to 22 Ω^{-1} cm^2 mol^{-1} for [*n*-Bu_4N][BF_4].[6]

Hydrogen peroxide is known to react with thioethers, especially in acidic non-hydroxylic solvents,[23] and thus the H_2O_2 produced in reaction 1 could react with free dms (produced in reaction 2) to give water and dmso:

$$H_2O_2 + \text{dms} \rightarrow H_2O + \text{dmso} \qquad (3)$$

As previously mentioned, apart from the spectra collected at $t = 0$ and $t = 2340$ min, all the rest exhibit a broad signal in the range $\delta \sim 6.2-7.1$. This signal initially shifts upfield from δ 6.6 to 6.25 and then shifts downfield while getting broader and less intense; after 1290 min it is just visible at $\delta \sim 7.1$. The signal is tentatively assigned to H_2O, H_2O_2, and the CO_2H proton of $PhCO_2H$, all rapidly exchanging with each other. The relative concentrations of these species would then determine the exact position of the resulting signal at a given time. Hydrogen peroxide could also react, but presumably less readily, with coordinated dms (other fates for H_2O_2, such as reaction with benzoic acid to form a peracid intermediate, cannot be ruled out, but there is no evidence to invoke such reactions). Typically reaction of H_2O_2 with thioethers results in coproduction of sulfone;[23] however, no sulfone is detected in the current case (a small quantity of sulfone is produced in the photoactivated O_2 oxidation of excess thioether catalyzed by Ru(OEP)(RR′S)$_2$[8]).

Ligand exchange between the species **1**, **2**, and **3** is fast relative to the observed rate of dms oxidation,[8] and so the concentrations of these species are determined by the relative affinity of free dms and dmso for *Ru*. Indeed, the quotient ([**2**][dms])/([**1**][dmso]) is essentially constant over the reaction time, with an average value of 70 ± 15 (Figure S2), which is comparable to the equilibrium constant of 16.7 ± 0.6 determined directly for the substitution of Et_2S by Et_2SO on $Ru^{II}(Et_2S)_2$.[8] For the equilibrium constant ([**3**][dms])/([**2**][dmso]), an estimate of 0.4 is obtained from the data set collected at $t = 1290$ min, close to the value of 0.37 ± 0.01 obtained independently for the analogous Et_2S/Et_2SO system.[8]

Figure 4 shows that, after the initial rapid oxidation step, the concentrations of the Ru^{III} species **4** and **5** gradually decrease (Figure 4b), while those of the Ru^{II} species **2** and **3** increase (Figure 4a). In the final spectrum of Figure 1, species **3** comprises about 90% of the product distribution (cf. Figure 4a). These data are not explained by eqs 1−3, which give no indication of how a net reduction of the Ru^{III} species is achieved after their initial production. Considerable insight into the mechanism of this gradual reduction of the Ru center came from unsuccessful attempts to prepare pure **5**. Figure 5a shows the ^{1}H NMR spectrum obtained for an approximately 1:1 mixture of **4** and [Me_4N][*Ru*($PhCO_2$)$_2$] (**6**) in CD_2Cl_2, while Figure 5b shows the spectrum of pure **6** for comparison.[6] The major signals in Figure 5a are attributable to the desired complex **5**, and some

(21) Chu, M. M. L.; Castro, C. E.; Hathaway, G. M. *Biochemistry* **1978**, *17*, 481.

(22) Sawyer, D. T.; Roberts, J. L., Jr. *Experimental Electrochemistry for Chemists*; John Wiley and Sons: New York, 1974; Chapter 4.

(23) Barnard, D.; Bateman, L.; Cuneen, J. I. In *Organic Sulfur Compounds*; Kharasch, N., Ed.; Pergamon Press: New York, NY 1961; Vol. I, Chapter 21.

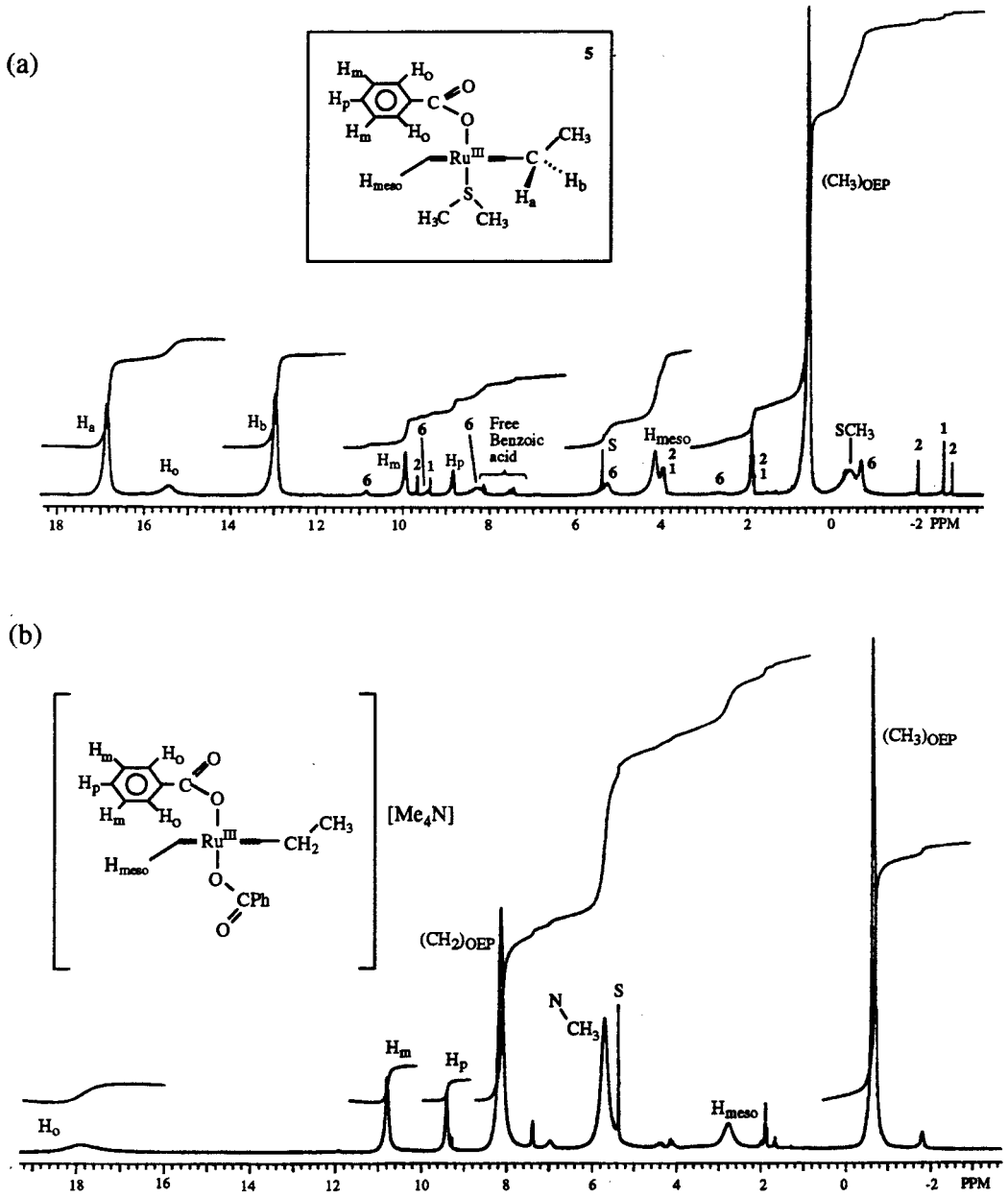

Figure 5. ^{1}H NMR spectra of (a) a mixture (approximately 1:1) of $[Ru(OEP)(dms)_2][BF_4]$ (**4**) and $[Me_4N][Ru(OEP)(PhCO_2)_2]$ (**6**) ~1 h after mixing and (b) pure **6**. Both spectra in CD_2Cl_2 at 20.0 °C, with samples sealed under vacuum; S = solvent.

signals due to residual **6** are also present because the original mixture was not exactly 1:1. The key feature is that Figure 5a also shows small approximately equal amounts of **1** and **2**. Attempts to crystallize out the desired product (**5**) from the mixture using hydrocarbon solvents resulted in a dramatic increase in the concentrations of the Ru^{II} species **1** and **2** in the isolated solid (this time with a predominance of **1**) and in the generation of other unidentified diamagnetic products (not shown).[8a] To account for the generation of **1** we speculate that a "disproportionation" such as the following takes place:

$$[Ru^{III}(dms)_2]^+ \,(\mathbf{4}) + Ru^{III}(dms)(PhCO_2)\,(\mathbf{5}) \rightleftharpoons Ru^{II}(dms)_2\,(\mathbf{1}) + [Ru^{IV}(dms)(PhCO_2)]^+ \quad (4)$$

Earlier CV studies[6] have shown that species **6**, with two coordinated benzoates, has a Ru^{IV}/Ru^{III} potential of 0.23 V, which almost exactly matches the Ru^{III}/Ru^{II} potentials of $[Ru(OEP)(RR'S)_2]^{+/0}$ complexes (0.22 V for the species in the presence of BF_4^- counterion).[6] The Ru^{IV}/Ru^{III} potential for **5**, containing a single benzoate, would certainly be higher than 0.23 V, but it must be in the range where the equilibrium (4) can be realized, although lying well to the left-hand side in CH_2Cl_2 solution. Such disproportionation of Ru^{III} into Ru^{II} and Ru^{IV} species is known.[24]

The oxidizing ability of Ru^{IV} species via Ru^{IV}=O intermediates as O-atom donors is well established within N_4-donor ligand systems,[25−27] and thus speculative pathways, such as Scheme 1, for the subsequent generation of the observed (**2**) product in Figure 5a are readily formulated. Here, the Ru^{IV}=O species presumably arises by deprotonation of coordinated OH; subse-

(24) Farrer, B. T.; Thorp, H. H. *Inorg. Chem.* **1999**, *38*, 2497.
(25) Griffith, W. P. *Chem. Soc. Rev.* **1992**, *21*, 179.
(26) Cheng, W.-C.; Yu, W.-Y.; Cheung, K.-K.; Che, C.-M. *J. Chem. Soc., Dalton Trans.* **1994**, 57 and references therein.
(27) (a) Binstead, R. A.; Stultz, L. K.; Meyer, T. J. *Inorg. Chem.* **1995**, *34*, 546 and references therein. (b) Stultz, L. K.; Binstead, R. A.; Reynolds, M. S.; Meyer, T. J. *J. Am. Chem. Soc.* **1995**, *117*, 2520 and references therein.

Scheme 1. Plausible Route for Oxidation of dms by Ru^{IV}

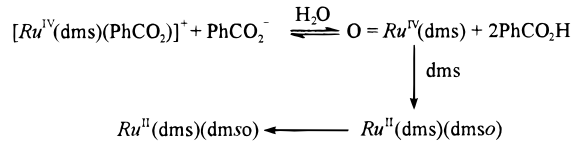

quent O-atom transfer to the thioether is well documented.[2,3] The conversion from O- to S-bonded dmso (linkage isomerization) is thought to occur in this system via stepwise dissociation/association of dmso,[8] although an intramolecular process via a π-bonded S=O moiety has been proposed for $[Ru(NH_3)_5(dmso)]^{2+}$.[28] In Figure 5a, trace H_2O in the solvent could be sufficient to generate the small quantities of **1** and **2** present. Presumably in the presence of hydrocarbons, additional mechanisms are operative in generating the large amounts of Ru^{II} products observed during the attempted crystallization procedures. The presence of such mechanisms suggests that as the solvent system becomes progressively less polar, the force driving Ru^{III} species towards Ru^{II} must become substantial.

According to eqs 1−3, the reaction being followed in Figure 1 will ultimately generate in situ 1 equiv of H_2O for every 2 equiv of Ru^{II} oxidized to Ru^{III}. Thus for this system, eq 4 and Scheme 1 combined provide a plausible route by which all of the Ru^{III} species could be reduced back to Ru^{II}. The presence of Ru^{IV} via equilibrium 4 could well explain the slight shifts observed in the signals of **5** toward the end of the stoichiometric oxidation reaction (cf. Figure 1), when [**1**] in particular has decreased to minimal levels. Furthermore, eq 4 and Scheme 1 provide a second route for dms oxidation to dmso, so that the sequence of reactions 1−4, followed by the reactions of Scheme 1, and dms/dmso ligand exchange processes, together give eventual formation of $Ru(OEP)(dmso)_2$, via the overall stoichiometry of eq 5.

$$Ru^{II}(OEP)(dms)_2 + O_2 \rightleftharpoons Ru^{II}(OEP)(dmso)_2 \qquad (5)$$

This net reaction shows that the benzoic acid is not consumed and acts as a catalyst, specifically to promote reaction 1; similarly water also acts as a catalyst, being formed in reaction 3 and consumed within Scheme 1. The mechanism implies that the oxygen of the dmso ligands comes via H_2O_2 (eqs 1 and 3) and H_2O (Scheme 1). Attempts to investigate the role of water more extensively, for example, by presaturating the CH_2Cl_2 with H_2O (or H_2O^{18}), were thwarted by the coproduction of significant amounts of $[Ru(OEP)L]_2O$ (L = anionic ligand) under these conditions.[8] Figure 6a shows in detail how the benzoate proton signal positions vary as the oxidation reaction progresses. It is immediately clear that at 2340 min the benzoate signals are shifted somewhat upfield from their position at $t = 0$. However, a comparable shift is observed if 1 equiv of dmso is added to a solution containing only benzoic acid (Figure 6b), which shows that such a shift is expected when benzoic acid interacts with dmso (presumably an acid−base interaction[29]). Thus the ^1H NMR results show that benzoic acid is recovered intact at the end of the oxidation reaction. At intermediate times, the H_m and H_p signals shift upfield and come closer together, behaviors also seen when comparing the ^1H NMR spectrum of the salt $[Me_4N][PhCO_2]$ with that of $PhCO_2H$.

One final point for consideration is the possible role of a species such as $[Ru^{III}(dms)(dmso)]^+$, which could be generated by ligand exchange as free dmso accumulates. Coordination of a sulfoxide to Ru^{III} makes the metal much more reducible than its thioether counterpart (e.g., the reduction potential for the $[Ru^{III}(dmso)_2]^+/Ru^{II}(dmso)_2$ couple is 0.74 V[6]); thus, if a species such as $[Ru^{III}(dms)(dmso)]^+$ is formed during the $Ru^{II}(dms)_2$ oxidation sequence, it will be rapidly and preferentially reduced to the Ru^{II} form, either in a "disproportionation" step analogous to eq 4, or via electron transfer from $Ru^{II}(OEP)(dms)_2$. However, CV data reveal a strong preference of Ru^{III} for thioether rather than sulfoxide coordination, implying that $[Ru^{III}(dms)(dmso)]^+$ species probably do not play an important role in the overall reaction. Figure 7 shows the CV of a solution containing primarily Ru^{II}(decMS)(decMSO) prepared by mixing 0.78 mM $Ru^{II}(decMS)_2$, 71 mM decMS, and 25 mM decMSO (cf. Figure 2; also, Ru^{II}(RR′S)(RR′SO) complexes have a λ_{max} at 403 nm, and this can be used to investigate the composition of the above mixture[8]). Initially, as the potential is scanned in the positive direction, a large signal attributed to the oxidation of Ru^{II}(decMS)(decMSO) is found at 0.59 V, and a minor signal attributed to $Ru^{II}(decMS)_2$ oxidation is found at 0.28 V. As the potential is scanned back in the negative direction, the 0.21 V peak due to $[Ru^{III}(decMS)_2]^+$ reduction is now the major one, while that at 0.50 V due to $[Ru^{III}$(decMS)(decMSO)$]^+$ reduction is comparatively minor. The observations are explained by the sequence given in Scheme 2, and show that thioether coordination to Ru^{III} is preferred over sulfoxide coordination. From Figure 7 $\Delta E°$ for reduction of $[Ru^{III}$(decMS)(decMSO)$]^+$ by $Ru^{II}(decMS)_2$ is found to be 0.3 V, which translates to an equilibrium constant of 10^5. As mentioned earlier (cf. also Figure S2), the equilibrium constants for replacement of aliphatic thioethers by sulfoxides in Ru^{II} species have magnitudes of ∼20−70. Combining the equilibrium constants for the two processes yields an expected value of $(2-7) \times 10^{-4}$ for the replacement of a thioether by a sulfoxide in $Ru^{III}(RR'S)_2^+$ species.

In summary, in CD_2Cl_2 containing $PhCO_2H$, O_2 initially oxidizes $Ru^{II}(dms)_2$ to a mixture of $[Ru^{III}(dms)_2]^+$ and $Ru^{III}(dms)(PhCO_2)$, apparently via an inner-sphere, acid-promoted step which also produces H_2O_2. The latter can oxidize dms to dmso, generating H_2O in the process. Subsequently, $[Ru^{III}(dms)_2]^+$ is reduced back to the corresponding Ru^{II} complex by $Ru^{III}(dms)(PhCO_2)$, whose oxidation potential has been lowered upon replacement of the coordinated thioether by benzoate. The $[Ru^{IV}(dms)(PhCO_2)]^+$ thus formed can react with the water produced in the H_2O_2 oxidation of dms, to give $O=Ru^{IV}(dms)$ and regenerate free $PhCO_2H$. Finally, like H_2O_2, $O=Ru^{IV}(dms)$ can also oxidize dms to dmso. The net reaction (eq 5) is thus oxidation of both dms ligands in **1** by 1 equiv of O_2. The mechanism may be compared to that proposed by Riley[30] for the O_2 oxidation of dms to dmso catalyzed by *cis*-$RuCl_2(dmso)_4$ in alcohols. Here, free H_2O_2 was suggested to be formed via an initial 2e O_2 oxidation of Ru^{II} with direct generation of Ru^{IV}; in our system, the detection of Ru^{III} strongly favors the 1e process followed by a disproportionation. Riley also considered reaction 6 for the subsequent reduction of Ru^{IV}

$$Ru^{IV}(dms) + H_2O \rightleftharpoons Ru^{II} + dmso + 2H^+ \qquad (6)$$

back to Ru^{II}; this is essentially the chemistry of Scheme 1, although we invoke the presence of a $Ru^{IV}=O$ intermediate. We prefer a pathway via this intermediate versus the previously proposed nucleophilic attack of water on dms,[30] because attack of a thioether at an electrophilic oxo center has been demonstrated[2,25,27] and, in our system, this provides the most obvious pathway to the detected mixed dms/dmso species **2**.

(28) Scott, A. Y. N.; Taube, H. *Inorg. Chem.* **1982**, *21*, 2542.
(29) Jaswal, J. S.; Rettig, S. J.; James, B. R. *Can. J. Chem.* **1990**, *68*, 1808.
(30) (a) Riley, D. P. *Inorg. Chem.* **1983**, *22*, 1965. (b) Riley, D. P.; Shumate, R. S. *J. Am. Chem. Soc.* **1984**, *106*, 3179.

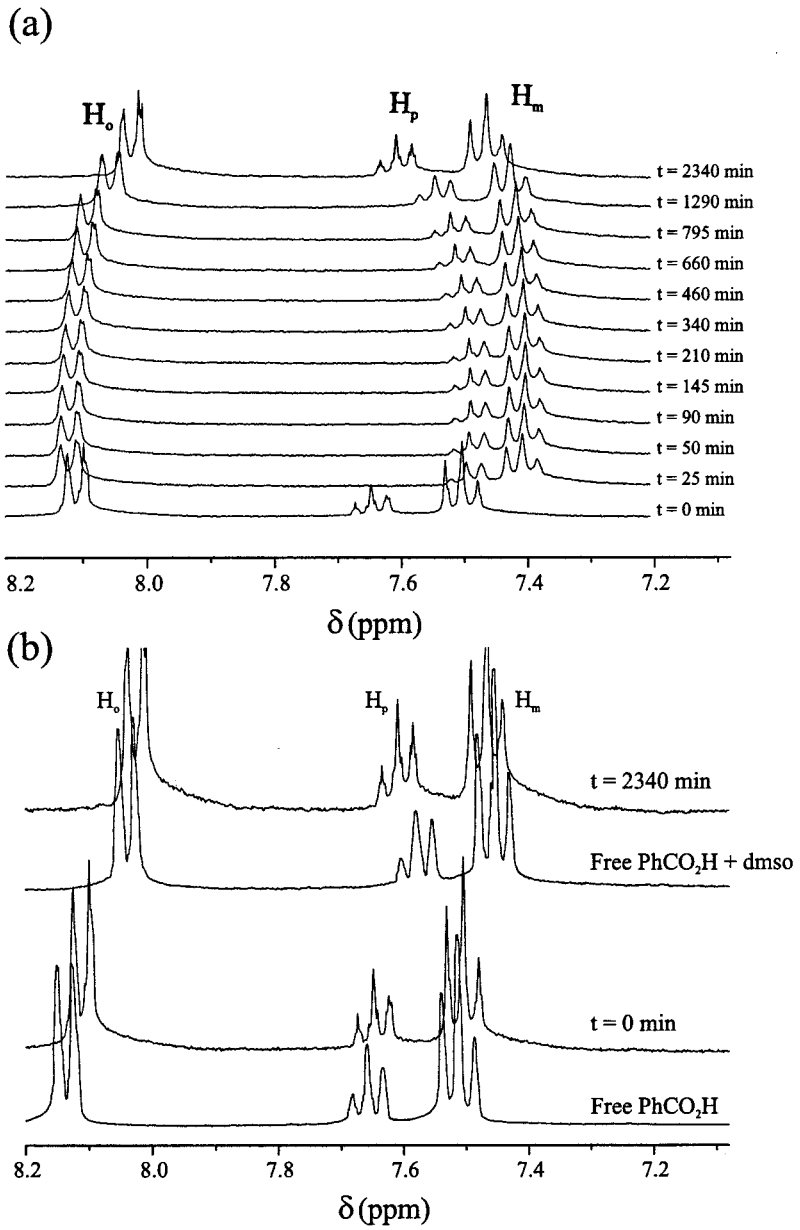

Figure 6. (a) Changes over time (min) in the ^{1}H NMR phenyl signals due to free benzoic acid and benzoate, for the same experiment as shown in Figure 1. (b) Comparison of the first and last spectra shown in Figure 6a with spectra of free benzoic acid in CD_2Cl_2, with and without an added equivalent of free dmso, in the absence of Ru(OEP) species.

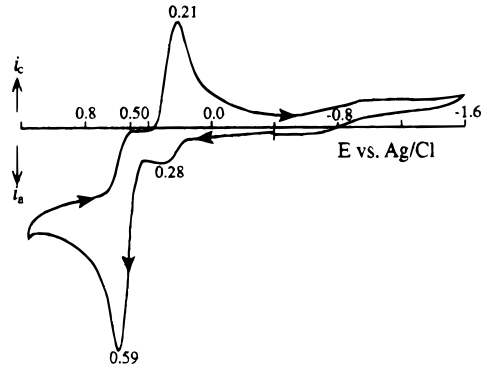

Figure 7. Cyclic voltammogram of a solution (CH_2Cl_2/[n-Bu_4N][BF_4]) initially containing 0.78 mM Ru(OEP)(decMS)$_2$, 71 mM decMS, and 25 mM decMSO.

Reaction of Ru(OEP)(RR′S)$_2$ Complexes with O_2 and $PhCO_2H$ in Hydrocarbon Solvents. In benzene or toluene containing $PhCO_2H$, exposure of *Ru*^{II}(dms)$_2$ or *Ru*^{II}(Et_2S)$_2$ to O_2, under conditions analogous to those described for the reactions in CH_2Cl_2, also results in the production of the *Ru* mono- and bis-sulfoxide complexes. The general mechanisms are probably similar, but the lower polarity of the hydrocarbon solvents (dielectric constant $\approx$ 2)[31] results in some minor, but interesting, differences. The reaction is much slower in hydrocarbons; e.g., after 35 h in a benzene solution otherwise analogous to the CH_2Cl_2 solution previously discussed, only

Scheme 2. Proposed Reactions for the Data of Figure 7

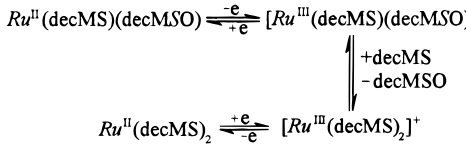

(31) *The Handbook for Chemistry and Physics*, 62nd ed.; Weast, R. C., Astle, M. J., Eds.; Chemical Rubber Company: Boca Raton, FL, 1981; pp E-53,54.

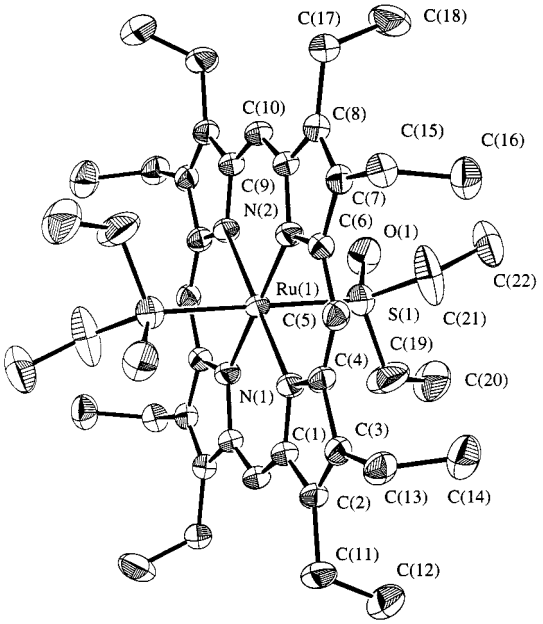

Figure 8. ORTEP view of Ru(OEP)(Et_2SO)$_2$. Disorder and hydrogen atoms are omitted for clarity; 33% thermal ellipsoids are shown.

Table 4. Selected Bond Lengths (Å) and Angles (deg) for Ru(OEP)(Et_2SO)$_2$

Ru(1)−S(1)	2.319(1)	Ru(1)−N(1)	2.062(3)
Ru(1)−N(2)	2.051(3)	S(1)−O(1)	1.508(4)
S(1)−C(19)	1.777(8)	S(1)−C(21)	1.776(9)
S(1)−Ru(1)−S(1)[a]	180.0	S(1)−Ru(1)−N(1)	91.8(1)
S(1)−Ru(1)−N(1)[a]	88.2(1)	S(1)−Ru(1)−N(2)	90.3(1)
S(1)−Ru(1)−N(2)[a]	89.7(1)	N(1)−Ru(1)−N(1)[a]	180.0
N(1)−Ru(1)−N(2)	90.3(1)	N(1)−Ru(1)−N(2)[a]	89.7(1)
N(2)−Ru(1)−N(2)[a]	180.0	Ru(1)−S(1)−O(1)	117.3(2)
Ru(1)−S(1)−C(19)	112.1(3)	Ru(1)−S(1)−C(21)	112.6(3)
O(1)−S(1)−C(19)	106.3(4)	O(1)−S(1)−C(21)	106.0(4)
C(19)−S(1)−C(21)	100.9(6)		

[a] Symmetry operation: $1 - x$, $1 - y$, $1 - z$.

~65% of *Ru*^{II}(dms)$_2$ (**1**) has reacted, and the product is mainly *Ru*^{II}(dms)(dmso) (**2**) with traces of bis(sulfoxide) (**3**), and *Ru*^{III}(dms)($PhCO_2$) (**5**). No [*Ru*^{III}(dms)$_2$]$^+$ is seen [the ^{1}H resonances for **1**−**3** in C_6D_6 are very similar to those in CD_2Cl_2 (Table 2), while some of those of **5** are shifted by up to 1.5 ppm[8a]. The implications are that, in the hydrocarbons, reaction 2 lies far to the right with a resulting decreased contribution from the "disproportionation" reaction (4). In the corresponding system with *Ru*^{II}(Et_2S)$_2$, the findings are similar in that no [*Ru*^{III}(Et_2S)$_2$]$^+$ is seen, although more significant amounts of *Ru*^{III}(Et_2S)($PhCO_2$) are observed.[8]

Crystal Structure of Ru(OEP)(Et_2SO)$_2$ (7). The synthesis of **7**, along with other Ru(OEP)(RR′*SO*)$_2$ complexes, from the [Ru(OEP)]$_2$ precursor has been described earlier;[6] the evidence for coordination via the S-atom of the sulfoxides was solely solid-state IR data (e.g., ν_{SO} 1105 vs 1001 cm^{-1} for free Et_2SO), with ^{1}H NMR data subsequently being ascribed to the species. The X-ray data for **7** confirm that the sulfoxide ligands are S-bonded (Figure 8). Selected bond lengths and angles are given in Table 4.

There is nothing remarkable about the structure, although it is perhaps the first for a metalloporphyrin containing an S-coordinated sulfoxide. The variable orientations for the ethyl groups of the OEP are commonly seen,[5] and the bond lengths and angles for the Ru(OEP) moiety are normal.[5,6] There is a plethora of structural data for non-porphyrin Ru^{II} S-bonded sulfoxide complexes,[32] but none, to our knowledge, of S-bonded Et_2SO systems; the complex [$RuBr_2$(NO)(Et_2SO)][μ-Br]$_2$ contains O-bound sulfoxides.[33] Nevertheless, S-bonded sulfoxides generally have geometry very similar to that of the corresponding free sulfoxide.[32] The geometry of the coordinated Et_2SO in **7** appears similar to that of the S-bonded Et_2SO in some Pt^{II} complexes,[34] which is close to tetrahedral at the S atom with an S−O bond length of 1.48 Å; the disorder problem in the Et_2SO ligands of **7**, however, precludes a more accurate comparison. The Ru−S bond length (2.319 Å) in **7** is in the range of 2.30−2.36 Å found generally for mutually *trans*-sulfoxides in non-porphyrin Ru^{II} systems.[32]

Worth noting is that structural data show that the phthalocyanine complex FePc(dmso)$_2$ (a tetraazaporphyrin species) has S-bonded sulfoxides,[35] while IR data again suggest S-bonded sulfoxides in RuPc(dmso)$_2$.[36] S-Bonded sulfoxide complexes (as judged by IR data) of the sterically hindered Ru(TMP) system have also been synthesized in this laboratory.[2] To our knowledge, the only other structurally characterized bis(sulfoxide) complexes of metalloporphyrins are of [Fe(OEP)(dmso)$_2$][PF_6][37] and bis(tetramethylene sulfoxide)(tetraphenylporphinato)iron(III) perchlorate,[38] where all the sulfoxides are O-bonded.

Summary

A mechanism is proposed for the stoichiometric O_2 oxidation of Ru(OEP)(RR′S)$_2$ complexes to Ru(OEP)(RR′*SO*)$_2$ in CH_2Cl_2 solutions containing $PhCO_2H$. The reaction is initiated by an inner-sphere process in which a one-electron transfer generates Ru^{III} and superoxide; the latter disproportionates to give H_2O_2 that oxidizes free dms, displaced from the [Ru^{III}(OEP)(RR′S)$_2$]$^+$ by substitution with benzoate. "Disproportionation" of the [Ru(OEP)(RR′S)$_2$]$^+$ and Ru(OEP)(RR′S)($PhCO_2$) species by a one-electron redox process generates a Ru^{IV} intermediate; this with water formed from the H_2O_2 oxidation of dms leads to the formation of a Ru^{IV}═O species that transfers oxygen to a second mole of free dms. The net reaction is catalytic in $PhCO_2H$ and water.

A crystal structure of Ru(OEP)(Et_2SO)$_2$ confirms that the sulfoxides are bonded via the S atoms.

Acknowledgment. We thank the Natural Sciences and Engineering Research Council of Canada for financial support and Johnson Matthey Ltd. and Colonial Metals Inc. for the loan of Ru.

Supporting Information Available: Tables of crystallographic data collection procedures and parameters, complete atomic coordinates and thermal parameters, bond distances and angles, torsion angles, and least-squares planes (Tables S1−S8); the complete ^{1}H NMR spectra (Figure S1) shown in part in Figure 1, and plots showing equilibrium quotients for [**5**][dms]/[**4**][$PhCO_2^-$] and [**2**][dms]/[**1**][dmso] (Figure S2). This material is available free of charge via the Internet at http://pubs.acs.org.

IC9908219

(32) (a) Yapp, D. T. T.; Rettig, S. J.; James, B. R.; Skov, K. *Inorg. Chem.* **1997**, *36*, 5635. (b) Calligaris, M.; Carugo, O. *Coord. Chem Rev.* **1996**, *153*, 83.
(33) Ferguson, J. E.; Page, C. T.; Robinson, W. T. *Inorg. Chem.* **1976**, *15*, 2270.
(34) (a) Kukuskin, V. Y.; Belsky, V. K.; Konovalov, V. E.; Shifrina, R. R.; Moiseev, A. I.; Vlasova, R. A. *Inorg. Chim. Acta* **1991**, *183*, 57. (b) Belsky, V. K.; Konovalov, V. E.; Kukuskin, V. Y. *Acta Crystallogr., Sect. C: Cryst. Struct. Commun.* **1993**, *C49*, 751.
(35) Calderazzo, F.; Pampaloni, G.; Vitali, D.; Collmati, I.; Dessy, G.; Fares, J. *J. Chem. Soc., Dalton Trans.* **1980**, 1965.
(36) Dolphin, D.; James, B. R.; Murray, A. J.; Thornback, J. R. *Can. J. Chem.* **1980**, *58*, 1125.
(37) Muthusamy, M.; Andersson, L. A.; Sun, J.; Loehr, T. M.; Thomas, C. S.; Sullivan, E. P., Jr.; Thomson, M. A.; Long, K. M.; Anderson, O. P.; Strauss, S. H. *Inorg. Chem.* **1995**, *34*, 3953.
(38) Mashiko, T.; Kastner, M. E.; Spartalian, K.; Scheidt, W. R.; Reed, C. A. *J. Am. Chem. Soc.* **1978**, *100*, 6354.